Clays and Clay Minerals, Vol. 55, No. 6, 543–553, 2007.

COMBINED NEAR-INFRARED AND X-RAY DIFFRACTION INVESTIGATION OF THE OCTAHEDRAL SHEET COMPOSITION OF PALYGORSKITE

VASSILIS GIONIS[1], GEORGE H. KACANDES[2], IOANNIS D. KASTRITIS[2] AND GEORGIOS D. CHRYSSIKOS[1,*]

[1] Theoretical & Physical Chemistry Institute, National Hellenic Research Foundation, 48 Vass. Constantinou Ave., Athens, Greece 11635

[2] Geohellas S.A., 60 Zephyrou Str., Athens, Greece 17564

Abstract—The octahedral composition of palygorskite in more than 300 samples from the Pefkaki deposit, W. Macedonia, Greece, has been studied by near-infrared (NIR) and X-ray diffraction (XRD), and evaluated according to the formula $y Mg_5Si_8O_{20}(OH)_2 \cdot x Mg_2Fe^{III}_2Si_8O_{20}(OH)_2 \cdot (1-x-y) Mg_2Al_2Si_8O_{20}(OH)_2$. Included in the study were PFl-1 and several commercial palygorskites. Our analysis of 2nd derivative NIR spectra shows that the dioctahedral composition is adequately described by three sharp overtone bands representing AlAlOH, $AlFe^{III}OH$ and $Fe^{III}Fe^{III}OH$ in *M*2 dioctahedral sites, and that the summed intensity of these bands is proportional to the amount of dioctahedral component present ($1-y$). The samples show large variations in the degree of dioctahedral Fe^{III}-for-Al substitution with Fe^{III} occupying up to 70% of the dioctahedral *M*2 sites. Ternary analysis shows that the distribution of dioctahedral Al and Fe^{III} is not random, but displays a tendency towards homoionic pairing. An overtone band at 7214 cm^{-1} and several combination bands are indicative of a trioctahedral Mg_3OH component (y), and their appearance correlates with a distinct palygorskite signature in thermogravimetric analysis. Nevertheless, these bands cannot be used reliably for the quantification of a trioctahedral palygorskite component due to their close similarity to those of sepiolite. To circumvent this problem, we have evaluated y indirectly by calculating the difference between $1-y$ and the total concentration of palygorskite determined by the normalized intensity of the d_{110} XRD peak of palygorskite at 10.4 Å. Using this methodology, we have found that the samples conform to a trioctahedral limit of $y \approx 0.55$, although within this limit they display large variations in octahedral character. Finally, we extend the above methodology to PLS chemometrics and show how NIR can be used to determine palygorskite content routinely in multimineralic geological samples.

Key Words—Greece, Near-infrared Spectroscopy, Octahedral Composition, Palygorskite, X-ray Diffraction.

INTRODUCTION

Palygorskite/sepiolite minerals are unique among clays in that they consist of 2:1 units with a modulated tetrahedral sheet (Brindley and Brown, 1980; Jones and Galán, 1988; Singer, 1989). The octahedral sheet is thus discontinuous, giving rise to alternating 2:1 'slabs' that are linked to each other through Si–O–Si bonds between adjacent SiO_4 tetrahedra. The gaps between slabs form tunnels that contain both zeolitic and crystalline water, the latter completing the coordination of Mg atoms at the edges of each octahedral sheet.

While sepiolite is thought to be uniformly trioctahedral and of orthorhombic symmetry (Post *et al.*, 2007), palygorskite can be either orthorhombic or monoclinic (Christ *et al.*, 1969; Artioli and Galli, 1994; Giustetto and Chiari, 2004) and can be assigned a variable dioctahedral–trioctahedral character expressed by the general formula

$$[M^{II}_{3x+2}M^{III}_{2(1-x)}\square_{1-x}]Si_8O_{20}(OH)_2(OH_2)_4.4H_2O$$

where M^{II} = Mg and M^{III} = Al, Fe (Paquet *et al.*, 1985; Galán and Carretero, 1999). The end-member structure of the octahedral sheet at $x = 0$ (dioctahedral) and $x = 1$ (trioctahedral) is shown in Figure 1 (adapted from Güven *et al.*, 1992).

Regardless of dioctahedral-trioctahedral character and symmetry considerations, the detection of palygorskite by XRD is based on the presence of a strong 110 line at ~10.4 Å, which is unaffected by either mild heat treatment (<200ºC) or ethylene glycol solvation (Moore and Reynolds, 1997). All other palygorskite diffraction peaks are weak and of little diagnostic value in the presence of other clay minerals.

Vibrational spectroscopy is suitable for determining the speciation of the octahedral sheet of smectites by taking advantage of the sensitivity of the hydroxyl stretching and bending modes on the nature and extent of cationic substitutions in the octahedral sheet (Zviagina *et al.*, 2004; Gates, 2005; Madejová and Komadel, 2005 and references therein). However, plausible interpretations of IR data addressing the composition of the octahedral sheet of palygorskite have been reported only very recently. Suárez and García-Romero (2006) studied the Fourier transform infrared (FTIR) spectra of six palygorskite samples of variable composition and

* E-mail address of corresponding author:
gdchryss@eie.gr
DOI: 10.1346/CCMN.2007.0550601

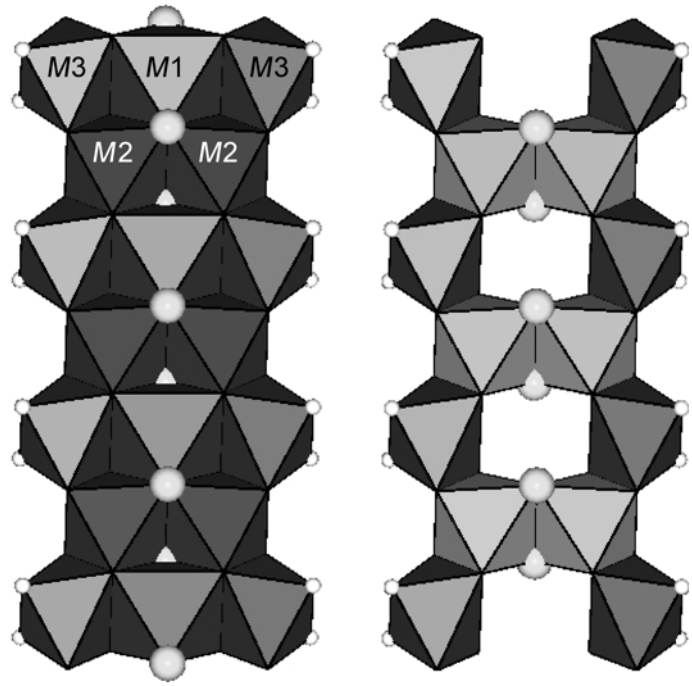

Figure 1. Idealized octahedral sheet of palygorskite. Small and large spheres depict bound H_2O and structural OH, respectively. In the trioctahedral end-member (left) all three octahedral sites are fully populated by bivalent cations (Mg) whereas the dioctahedral analog (right) has vacant *M*1 sites, trivalent ions (Al, Fe) in *M*2 sites, and Mg in *M*3 sites.

reported that isomorphic substitutions by trivalent Al and Fe ions can take place only in the *M*2 (inner) sites, whereas Mg can occupy all three sites (*M*1, *M*2 and *M*3). Inspired by the seminal work of Clark *et al.* (1990), Gionis *et al.* (2006) combined NIR and mid-infrared (MIR) attenuated total reflectance (ATR) spectroscopies to study the structure of PFl-1, The Clay Minerals Society Source Clay from Gadsden County, Florida, and Gr-1, a palygorskite from the newly discovered Pefkaki deposit from W. Macedonia, Greece. Both clays were found to be almost exclusively dioctahedral and a self consistent set of assignments was established for the deformation, stretching, combination and overtone bands of dioctahedral AlAlOH, $AlFe^{III}OH$ and $Fe^{III}Fe^{III}OH$ species in ambient and dehydrated (130ºC) palygorskite.

Near-infrared spectroscopy offers many advantages for the systematic investigation of palygorskite-containing clays, in addition to providing a simple and non-destructive way of acquiring high signal-to-noise ratio spectra. The hydrous clay fraction of a sample can be studied in the presence of large amounts of non-clay minerals without the need to employ separation techniques because most anhydrous minerals, including silicates, have very weak absorption in the NIR region. In addition, the anharmonicity coefficients of the stretching modes of the structural OH groups are typically smaller than those of H_2O. As a result, NIR offers a better separation of the OH and H_2O modes compared to MIR. Due to the sharpness of the palygorskite NIR spectrum (Clark *et al.*, 1990), this separation can be further enhanced if 2^{nd} derivative analysis is employed to eliminate broad features due to water or other clays, as well as background effects (Gionis et *al.*, 2006).

Based on the above, this work reports on the NIR spectroscopic investigation and structural characterization of a large number of palygorskite-containing samples from the Pefkaki deposit of the Ventzia continental basin, W. Macedonia, Greece. This deposit consists of series of palygorskite, smectite and mixed palygorskite-smectite beds and is believed to have formed by diagenetic alteration of saprolitic sediments derived from the Vourinos ophiolite complex (Kastritis *et al.*, 2003). The aim of this paper is to probe the broad compositional variability of the octahedral sheet of palygorskite from one location, and compare it to the analytical data on individual particles from the literature. In doing so we combine NIR with XRD, both techniques that can be applied routinely with minimum sample preparation, and can therefore find practical application for the systematic evaluation of clay deposits.

MATERIALS AND METHODS

More than 300 samples of palygorskite-bearing clay were collected from 20 drill cores from the Pefkaki deposit. In addition to palygorskite, other minerals present include saponitic smectite, serpentine (lizardite and/or antigorite), quartz, calcite, dolomite and kaolinite. Included in the comparisons are PFl-1 (CMS Source

Clay, Gadsden County, Florida), Gr-1 (Pefkaki deposit; Gionis *et al.*, 2006), and nine commercial samples of unsubstantiated provenance from clay companies in the USA and China. The commercial samples contain 50–90% attapulgite and variable amounts of smectite, quartz, calcite and dolomite.

In preparation for analysis, the Pefkaki samples were dried in air at ambient conditions (T = 25±3ºC, RH = 30±5%) and ground to <250 μm using a Retsch hammer mill. The NIR analyses were conducted on the ground material without further treatment. For XRD, the samples were ground for an additional 6 min in isopropanol using a McCrone micronizing mill.

Powder XRD data were obtained on randomly oriented powders using a Thermo ARL diffractometer (Model X'TRA 17) equipped with a Peltier detector and employing CuKα radiation at 45 kV and 40 mA. The divergence and receiving slits were 0.4 and 0.5 mm, respectively. The scans were conducted from 2 to 70º2θ using a step size of 0.04º2θ and a counting time of 2 s. Selected scans shown in this paper were conducted using a 0.02º2θ step size and a counting time of 10 s. A 12-position sample changer was used to accommodate 11 clay samples plus a quartz reference. The intensity of the 110 reflection of palygorskite was determined by measuring the peak height above background at the maximum near 10.4 Å. The intensities were normalized to the intensity of the 101 reflection of quartz from the same sample set, to account for instrumental effects. Such peak-height measurements were found to be reproducible within ~10%. No corrections were made for variations in sample mass absorption coefficient.

Near-infrared spectra (4000–8000 cm^{-1}) were measured using a Fourier transform spectrometer (Vector 22N by Bruker Optics), equipped with a bifurcated fiber optic bundle accessory (IN 261 by Bruker Optics). This accessory is suitable for the diffuse reflectance measurement of powders. All spectra were measured against a Spectralon® (Labsphere Inc.) reference. Selected samples were measured over a broader wavenumber range (3650–8000 cm^{-1}) against a gold mirror for reference, using an integrating sphere attachment on the same spectrometer.

Three 100-scan NIR spectra were acquired per sample and averaged. The resolution was 4 cm^{-1} and a zero-filling-factor of 2 was employed. Peak intensities were measured on 2nd derivative spectra, calculated by the Savitzky-Golay algorithm (Savitzky and Golay, 1964) with 13-point smoothing. The intensities were measured on the 2nd derivative spectra from the baseline at y = 0 and were found to be reproducible within ~5%. Partial least-squares (PLS) modeling was based on subroutines available in the Opus Quant2 software (Bruker Optics).

Thermogravimetric (TGA) data were obtained using a TGA Q500 analyzer (TA Instruments). To establish a standard initial moisture content, the samples were equilibrated overnight in a desiccator over $CaCl_2$. At the start of the analysis, a 10±1 mg sample was equilibrated at 40ºC in the platinum holder until a stable mass was obtained. Scans were conducted from 40 to 600ºC at a rate (h) of 10ºC/min under a blanket of flowing dry nitrogen (60 mL/min). Higher-resolution data at intermediate temperatures were obtained by equilibrating 25 mg of sample at 130ºC and heating to 300ºC at h = 2ºC/min.

RESULTS AND DISCUSSION

The 2nd derivative spectra of 70 clay samples from the Pefkaki deposit are compiled in Figure 2. Three characteristic ranges corresponding to the overtones of the OH-stretching modes (7300–6850 cm^{-1}), the combination bands of H_2O (5450–5050 cm^{-1}) and the stretching-deformation combinations of OH (4575–4150 cm^{-1}) are shown. The Savitzky-Golay 13-point smoothing was chosen to eliminate the relatively broad overtone spectra of H_2O (7300–6000 cm^{-1}). The main assignments of the observed diagnostic bands (Table 1) are based on Post and Borer (2000), Gates (2005), and Gionis *et al.* (2006). The derivative spectra indicate that the samples consist of dioctahedral palygorskite,

Table 1. Assignments of the diagnostic NIR bands (cm^{-1}).

2ν(OH)	
7240	Srp
7214	Sep or trioctahedral Pal Mg_3OH
7184	Sap Mg_3OH
7170	Srp
7151	Sap Mg_2FeOH
7056	Pal, dioctahedral AlAlOH
6994	Pal, dioctahedral $AlFe^{III}OH$
6928	Pal, dioctahedral $Fe^{III}Fe^{III}OH$
(ν+δ) H_2O	
5320	Pal, surface, coordinated to SiOH
5240	Pal or Sm
5200	Pal, coordinated and zeolitic
(ν+δ) OH	
4527	Kln
4503	Pal, dioctahedral AlAlOH
4464	Srp
4431	Pal, dioctahedral $AlFe^{III}OH$
4403	Srp
4365	Sep or trioctahedral Pal
4355	Pal, dioctahedral $Fe^{III}Fe^{III}OH$
4322	Sep or trioctahedral Pal
4303	Srp
4277	Srp
νOH + lattice M_{oct}-O-Si	
4251	Pal, dioctahedral, Fe^{III}-rich
4215	Pal, dioctahedral, Fe^{III}-rich
4187	trioctahedral Mg_3OH (Sap, Sep, or Pal)

Srp: serpentine; Sap: saponite; Pal: palygorskite

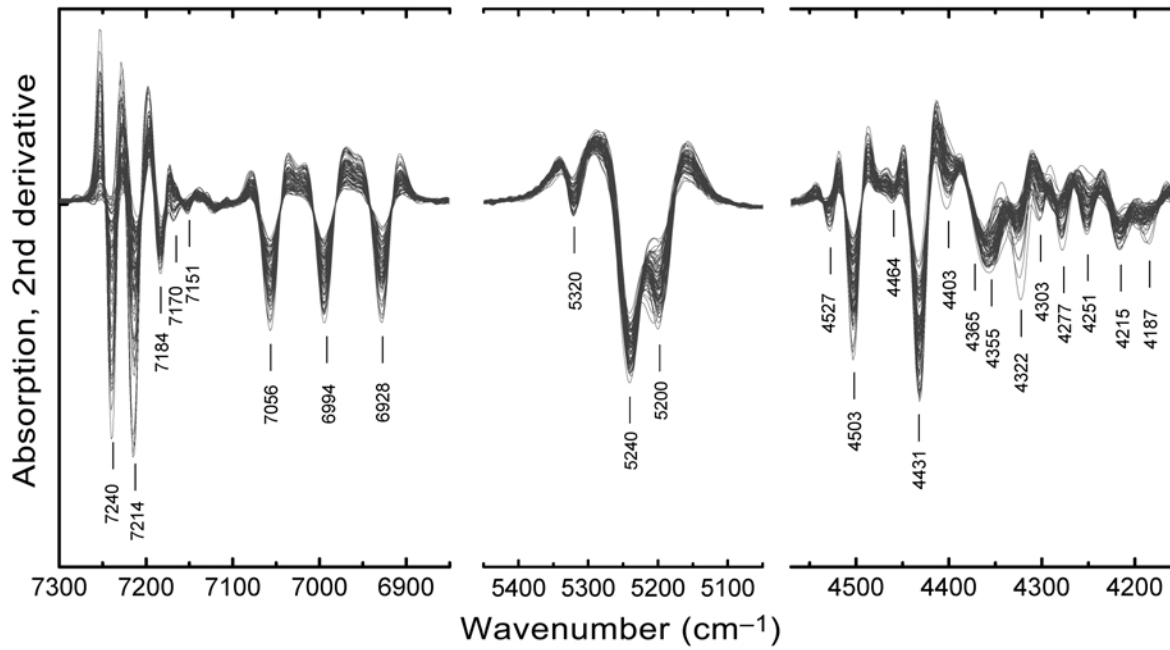

Figure 2. 2nd derivative NIR spectra of 70 palygorskite-bearing drill-core samples from the Pefkaki deposit.

serpentine, trioctahedral smectite (saponite), and trace kaolinite. In addition, an overtone band at 7214 cm^{-1} and several combination bands provide strong evidence for the presence of a trioctahedral palygorskite/sepiolite phase. The corresponding XRD spectra (not shown) confirm the presence of palygorskite, serpentine, a 14.8 Å smectite and minor quartz and chlorite, while kaolinite and sepiolite are below detection limits.

The dioctahedral 2ν(OH) overtone triplet of palygorskite is clearly seen at 7056, 6994 and 6928 cm^{-1}. The three components are observed at fixed wavenumbers over the whole sample set (*cf.* Gionis *et al*., 2006). They are separated by 62−65 cm^{-1} and have identical bandwidths of 36±1 cm^{-1} as determined from the distance between the zero-crossings around each 2nd derivative minimum. Therefore, these components are fully resolved in the 2nd derivative spectra under the resolution and smoothing conditions employed, and their relative intensities can be measured without interference effects. Gionis *et al.* (2006) have shown that the three components have the same anharmonicity parameters (X = 87±1 cm^{-1}, x_e = 0.023). Thus, it is reasonable to assume that the O−H stretching modes involved have very similar extinction coefficients, in agreement with Gates (2005) and others.

The relative intensities of the triplet components, normalized to their sum intensity, are shown in the ternary plot of Figure 3 for a subset of 180 samples containing >20% palygorskite. PFl-1, as well as the nine commercial samples of unknown origin are included in the comparison. Assuming that the components of the triplet have identical extinction coefficients (see above), the locus of each sample in the triangle allows for the direct evaluation of the relative population of the dioctahedral pairs AlAl, $AlFe^{III}$ and $Fe^{III}Fe^{III}$. For example, the dioctahedral signature of sample A in Figure 3 would consist of 55% AlAl, 31% $AlFe^{III}$ and 14% $Fe^{III}Fe^{III}$ pairs. The corresponding pair populations for sample B and PFl-1 are 16%, 30%, 54% and 86%, 10%, 4%, respectively. From these relative pair populations it is possible to calculate the Al and Fe^{III} cation occupancies in the dioctahedral *M*2 sites. For example, the Al occupancy of sample A would be (0.55 + 0.31/2) = 0.71 and the corresponding Fe^{III} occupancy (0.31/2+0.14) = 0.29. Thus, the spread of the points in Figure 3 corresponds to Al populating 30−91% of the dioctahedral *M*2 sites, with the remaining 9−70% being Fe^{III}. Within this range, PFl-1 is the most aluminous with 91% Al, while the Pefkaki samples vary between 30 and 70% Al. This analysis does not take into account a possible participation of Mg in the formation of dioctahedral pairs (AlMgOH, Fe^{III}MgOH or MgMgOH) because the NIR spectra show no evidence for their presence. This lack of evidence is in agreement with the MIR studies of Chahi *et al.* (2002) and Suárez and García-Romero (2006).

Interestingly, the locus of the $AlFe^{III}$OH component in the ternary plot is limited by a depressed arc, possessing considerably less curvature than would be indicated by an ideal statistical distribution of Al and Fe^{III} in the dioctahedral sites of palygorskite (solid and dotted arcs, respectively, Figure 3). The reduced amount of mixed $AlFe^{III}$ occupancy (Figure 3) indicates a chemical preference for the formation of AlAl and $Fe^{III}Fe^{III}$ homoionic pairs in dioctahedral palygorskite. A similar tendency towards homoionic pairing was

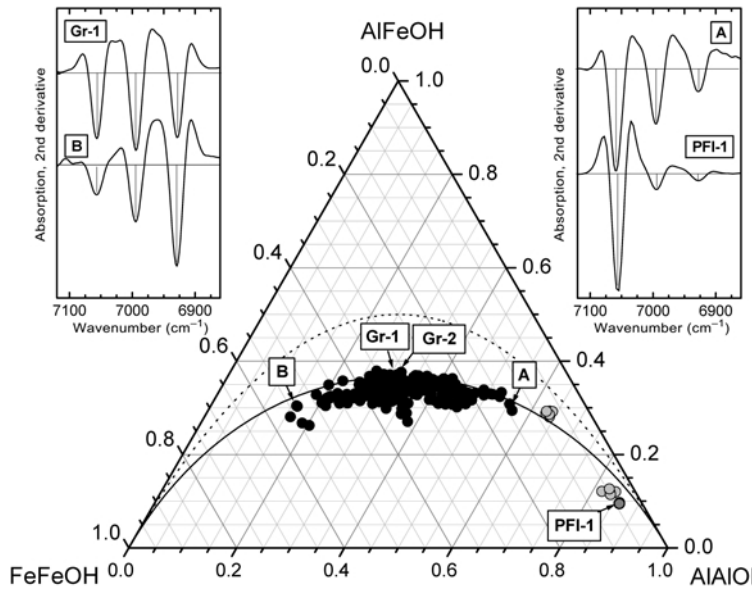

Figure 3. Occupancy of the *M*2*M*2 dioctahedral pairs of palygorskite by AlAlOH, $AlFe^{III}OH$ and $Fe^{III}Fe^{III}OH$. 177 Pefkaki samples containing >20% palygorskite (black), nine commercial samples of unknown origin (light gray) and PFl-1 (dark gray) are shown. The solid arc is a guide through the experimental points and the dotted arc corresponds to the statistical distribution of Al and Fe^{III} in the *M*2*M*2 pairs. Insets show details of the 2nd derivative spectra of characteristic samples, and define how intensities have been measured.

observed previously in dioctahedral smectite by Petit *et al.* (1995).

Two additional comments can be made based on simple mathematical considerations. (1) A mixture of two dioctahedral palygorskites with different Al occupancies, *i.e.* located on different positions of the depressed arc (Figure 3), would appear below the arc and on the chord linking the loci of the end members. This has been tested experimentally on artificial mixtures, and is probably the reason for some scatter of the data below the arc. (2) The depression of the arc does not change if the AlAlOH and $Fe^{III}Fe^{III}OH$ modes are assumed to have different extinction coefficients, provided that the extinction coefficient of the $AlFe^{III}OH$ mode is the average of those of its homoionic counterparts.

In an attempt to estimate the total dioctahedral palygorskite content of the Pefkaki samples, we have summed the 2nd derivative band intensities of the three dioctahedral overtone bands and normalized this value to that for sample Gr-1 (Gionis *et al*., 2006), assuming that GR-1 represents a pure palygorskite with 100% dioctahedral character. In Figure 4, we compare this NIR-based estimate to that determined independently from the XRD data on the same samples, where the XRD estimate was obtained by normalizing the intensities of the 10.4 Å peak of each sample to that measured for Gr-1. Most of the Pefkaki samples fall below the line that would correspond to a 1:1 correlation between the dioctahedral signature of NIR and the intensity of the 110 XRD peak for palygorskite. This scatter of data would result in NIR underestimating the palygorskite content of many samples by as much as ~50%. The overall correlation could not be improved by assigning different extinction coefficients for the AlAlOH and $Fe^{III}Fe^{III}OH$ modes. Instead, we observe that the extent of the deviation is proportional to the intensity of the 7214 cm^{-1} peak in the trioctahedral OH overtone range of the NIR spectra (Figure 2). Normally, this band is attributed to the Mg_3OH overtone stretch of sepiolite (Clark *et al*., 1990). However, the lack of a

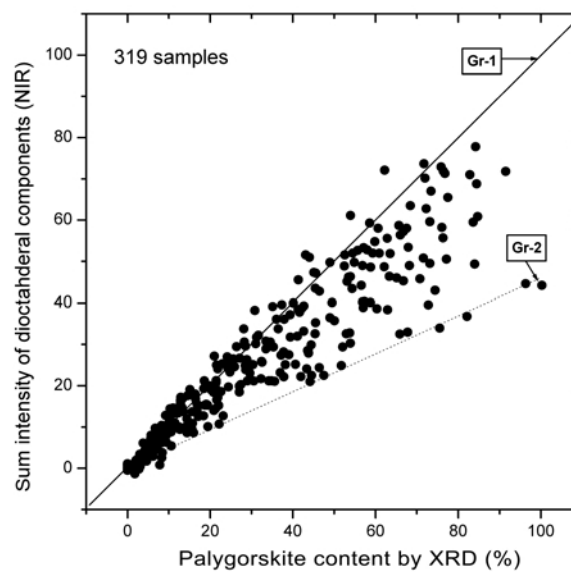

Figure 4. Correlation between the dioctahedral and total palygorskite contents of the Pefkaki samples estimated from the NIR and XRD data, respectively, and normalized to palygorskite Gr-1. The lines are used to help guide the eye. For details see the text.

detectable 12.0 Å feature in the XRD spectra suggests the assignment of the 7214 cm^{-1} band to trioctahedral palygorskite.

If the above assignment is correct, then the spread of the data in Figure 4 is due to the presence of trioctahedral palygorskite. Hence, one can employ XRD to estimate the total palygorskite content of the sample and NIR for estimating both dioctahedral palygorskite content and dioctahedral Al-Fe^{III} speciation. Ignoring H_2O and tetrahedral substitution, a palygorskite of mixed dioctahedral-trioctahedral character can be described by the general formula: $y Mg_5Si_8O_{20}(OH)_2 \cdot x Mg_2Fe^{III}_2Si_8O_{20}(OH)_2 \cdot (1-x-y)Mg_2Al_2Si_8O_{20}(OH)_2$ and depicted on a ternary diagram. The distribution of the Pefkaki samples containing >20% palygorskite by XRD is shown in Figure 5. The base corresponds to pure dioctahedral palygorskite of variable Al and Fe^{III} content (Mg = 2 per Si_8O_{20} in *M*3 sites and Al + Fe^{III} = 2 in *M*2 sites) as in Figure 3, but $y > 0$ positions indicate partially trioctahedral material with Mg occupying triplets of *M*1*M*2*M*2 sites in addition to the outer *M*3 sites (Figure 1). Clearly, the presence of trioctahedral palygorskite in the Pefkaki deposit is not related to the Fe^{III} content because the samples with large trioctahedral contents are distributed quite evenly among aluminous and ferric compositions, creating a trapezoidal cluster. Moreover, the maximum trioctahedral fraction of palygorskite reaches a limit of ~55%. As a result, the total number of octahedral cations per Si_8O_{20} in the Pefkaki palygorskites, determined solely from NIR and XRD data, ranges between 4 (Al+Fe^{III} = 2, 0.3 < Al/(Al+Fe^{III}) < 0.7, Mg = 2, M^{III}/M^{II} = 1) and 4.6 (Al+Fe^{III} = 0.88, Mg = 3.68, M^{III}/M^{II} = 4.2). Within this range, there is no evidence for the presence of compositional gaps.

Interestingly, a compilation of 28 selected palygorskite samples with reliable bulk chemical analysis data by Galán and Carretero (1999) indicates a very similar trioctahedral limit for palygorskite with two samples from Mt Flinders, (Queensland, Australia) and Dornboom, (South Africa) having Al+Fe^{III} = 0.82 and 0.68, Mg = 3.69 and 3.65, respectively. The bulk composition of a palygorskite from Ganntour, Morocco, studied by Chahi *et al.* (2002), corresponds to Al+Fe^{III} = 1.52 and Mg = 2.6, while a Mg-rich palygorskite from Guanshan (Anhui, China) is reported to have Al+Fe^{III} = 0.95 and Mg = 3.43 (Cai *et al*., 2007).

Previously, Paquet *et al.* (1985) published single-particle energy dispersive X-ray (EDX) analytical data on two palygorskite-containing clay fractions from Laval St. Roman and Jocas, France. In both samples, the octahedral composition of the palygorskite particles varies over very broad ranges, and the trioctahedral limit per Si_8O_{20} is Al+Fe^{III} = 0.9 and Mg = 3.85. More recently, García-Romero *et al.* (2004) reported the structural formula of a Mg-rich palygorskite from Esquivias, Spain, based on individual-particle EDX data. The average octahedral composition of this sample is Al+Fe^{III} = 1.24, Mg = 3.11, 19 of the 20 individual particle compositions studied falling below the upper limit of the trioctahedral component of the Pefkaki samples. For comparison, Figure 5 includes individual particle compositions of the Esquivias palygorskite, three Mg-poor palygorskites from Attapulgus (Georgia, USA), Bercimuel (Segovia, Spain) and Torrejón el Rubio (Cáceres, Spain) reported by García-Romero *et al.* (2004), as well as the data from

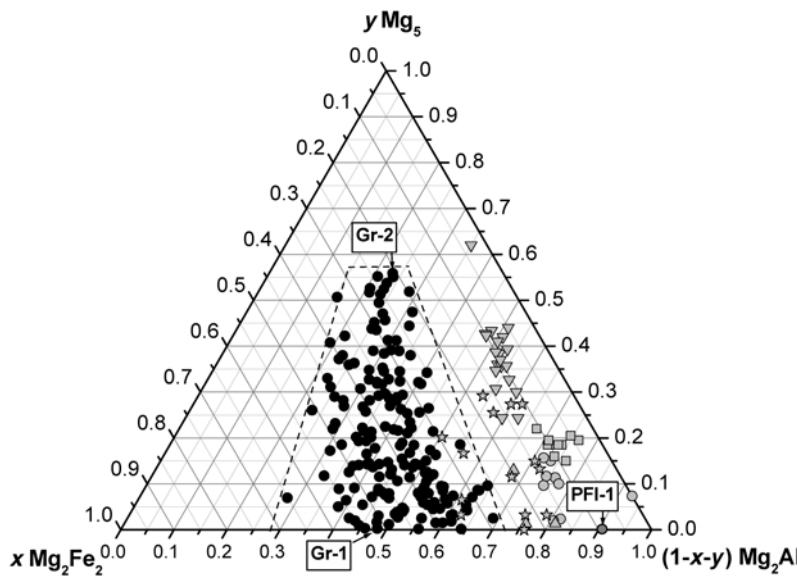

Figure 5. Distribution of trioctahedral, aluminous and ferric dioctahedral palygorskite in 177 Pefkaki samples with >20% palygorskite ●. Individual palygorskite particle analytical data (García-Romero, 2004; Chahi *et al.*, 2002) for the Esquivias ▽, Attapulgus ○, Bercimuel △, Torrejón □, and Ganntour ☆ samples are included for comparison.

Chahi *et al.* (2002) on the Ganntour (Morocco) sample. Interestingly, some of these sets of particles exhibit a compositional variability comparable to that of the whole Pefkaki sample set.

At the upper limit of trioctahedral palygorskite content, the Pefkaki sample set includes a pure sample, with minor chlorite and quartz admixtures, depicted as Gr-2 in Figures 3–5. The XRD spectrum of Gr-2 (Figure 6) is very similar to that of Gr-1 (Gionis *et al.*, 2006), and shows no trace of sepiolite at ~12 Å. The 110 peak of Gr-2 is shifted slightly to larger *d* values compared to Gr-1, and skewed. This trend has been observed in other Pefkaki palygorskites with a large trioctahedral fraction. A recent XRD investigation of palygorskites reports 110 positions ranging from 10.30 to 10.57 Å (Post and Crawford, 2007), but these do not appear to correlate with the Mg content of the samples. Martin Vivaldi and Linares Gonzalez (1962) reported the presence of a palygorskite-type clay from Cabo de Gata (Almeria, Spain), with a broad diffraction peak at ~11 Å, *i.e.* intermediate between palygorskite and sepiolite, and tentatively attributed to a random intergrowth of palygorskite and sepiolite. None of the Pefkaki samples exhibits this unusual behavior.

The TGA data on Gr-2 (Figure 7) indicate that this palygorskite exhibits a complex dehydration signature in the 100–300ºC temperature range, with overlapping events at ~210 and 230ºC. This is to be compared with a single event at 205ºC for dioctahedral Gr-1 (and PFl-1, Gionis *et al.*; 2006), and is clearly distinguished from sepiolite SepSp-1, where the corresponding events are observed above 250ºC. Frost and Ding (2003) reported TGA data on a number of palygorskite and sepiolite samples of different origins. Though distinguishing palygorskite from sepiolite, the data provided by these authors do not allow us to identify weight-loss events specific to trioctahedral palygorskite.

Despite the lack of XRD and TGA evidence for sepiolite in Gr-2, the NIR spectrum of Gr-2 exhibits trioctahedral characteristics that are nearly identical to SepSp-1, in all frequency regions of interest (Figure 8). The trioctahedral Mg_3OH stretch of Gr-2 and SepSp-1 have nearly identical anharmonicity constants (X = 84 and 83±1 cm^{-1}, respectively), compared to 84–86 cm^{-1} for magnesian talc (Petit *et al.*, 2004). One may notice that both the fundamental and first overtone Mg_3OH stretching vibrations of Gr-2 appear at slightly higher wavenumbers than those of SepSp-1. However, these differences are of limited diagnostic value until they are confirmed on a large set of sepiolite-containing samples and the dependence of the trioctahedral spectrum on hydration is investigated. At the current level of our understanding, Gr-2 cannot be distinguished by NIR from a suitable mixture of dioctahedral palygorskite Gr-1 and sepiolite SepSp-1.

As there is no XRD evidence for the presence of sepiolite in our samples, it is possible to revisit palygorskite content by NIR and XRD by taking into account the evidence for trioctahedral species, in addition to the dioctahedral component shown in Figure 4. In doing so, the intensity of the 7214 cm^{-1} band (defined as the distance of the 2nd derivative spectrum from the y = 0 baseline) is normalized to that of SepSp-1. A small correction equal to 0.17 times the

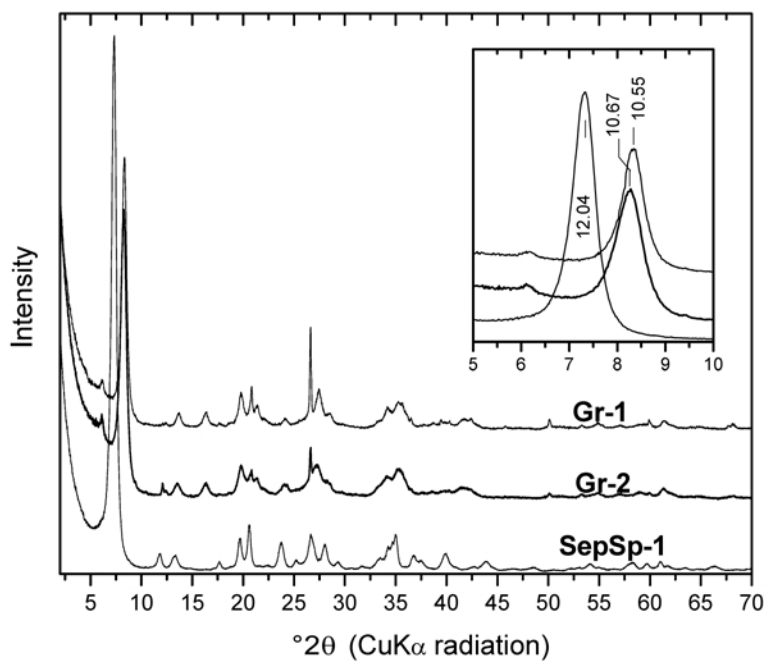

Figure 6. XRD patterns of palygorskite Gr-2 in comparison to Gr-1 from Gionis *et al.* (2006) and SepSp-1.

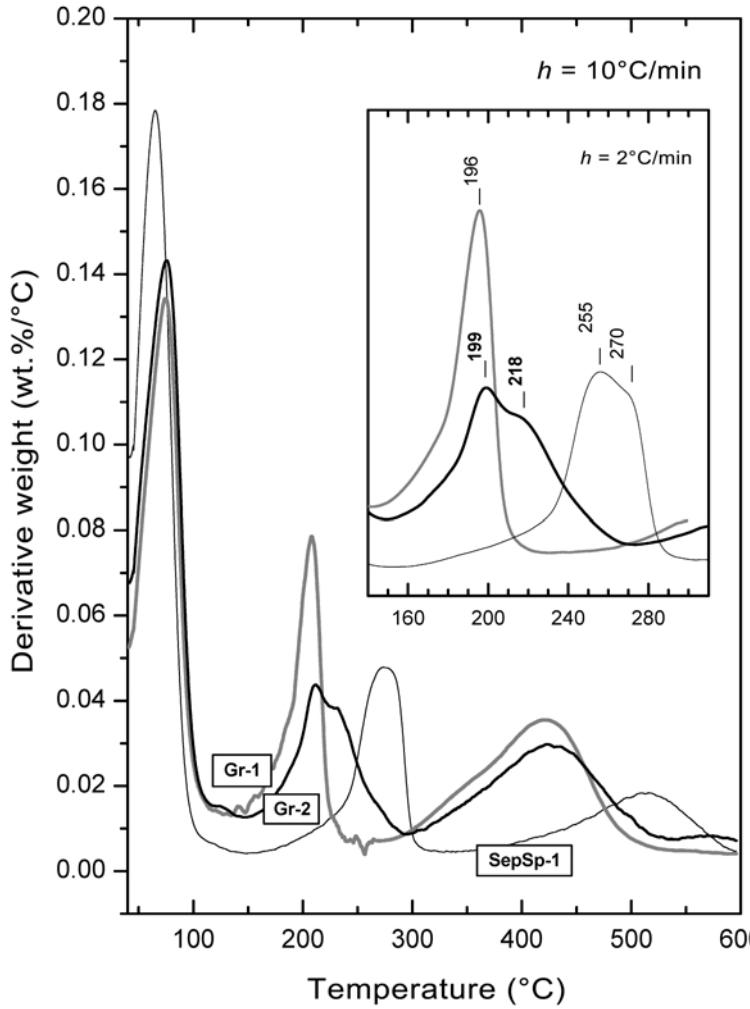

Figure 7. Derivative TGA traces of Gr-1, SepSp-1 and Gr-2. Heating rate: 10ºC/min. Inset: traces of the same samples measured at 2ºC/min.

intensity of the main serpentine overtone at 7240 cm^{-1} (Figure 2) is necessary to account for the effect of a minor band of this mineral that becomes significant in serpentine-rich Pefkaki samples. The resulting correlation between the NIR and XRD data (Figure 9, R^2 = 0.93, s.d. = 6.5) is clearly superior to that shown in Figure 4, confirming that trioctahedral palygorskite is an important component of many Pefkaki samples.

As a further improvement, it is possible to employ partial least-squares regression (PLS) in order to predict the total palygorskite content of the Pefkaki samples, defined previously on the basis of relative XRD intensities, from their NIR spectra. The PLS is a multivariate chemometric technique (Heise and Winzen, 2002), where a set of spectra (here, the 2nd derivative of the NIR absorption in the 4200−7300 cm^{-1} range, Figure 2) and a corresponding set of independent measurements (here, the total palygorskite content estimated from the XRD data) are analyzed to produce a function that allows for the prediction of the latter from the former. As such, PLS is more powerful than methods relying on the absolute intensity of a few diagnostic NIR bands (such as those shown in Figures 4 and 9). Also, PLS draws information not only from the presence of spectral features that correlate positively with the property of interest, but also from the absence of those that correlate negatively (such as the spectrum of the associated minerals in the Pefkaki deposit). The function is approximated by a linear combination of terms (ranks, vectors). These are calculated in order of decreasing importance. The number of ranks depends on the complexity of the system and the amount of relevant information that can be extracted from the spectra. Increasing the number of ranks improves predictions, but this increased dimensionality should not be used to fit noise (overfitting). It is therefore necessary to optimize the number of ranks (validation). One way of validating a PLS method involves splitting the total sample set in two subsets; one used for calibration and the other for testing this calibration by minimizing the root mean

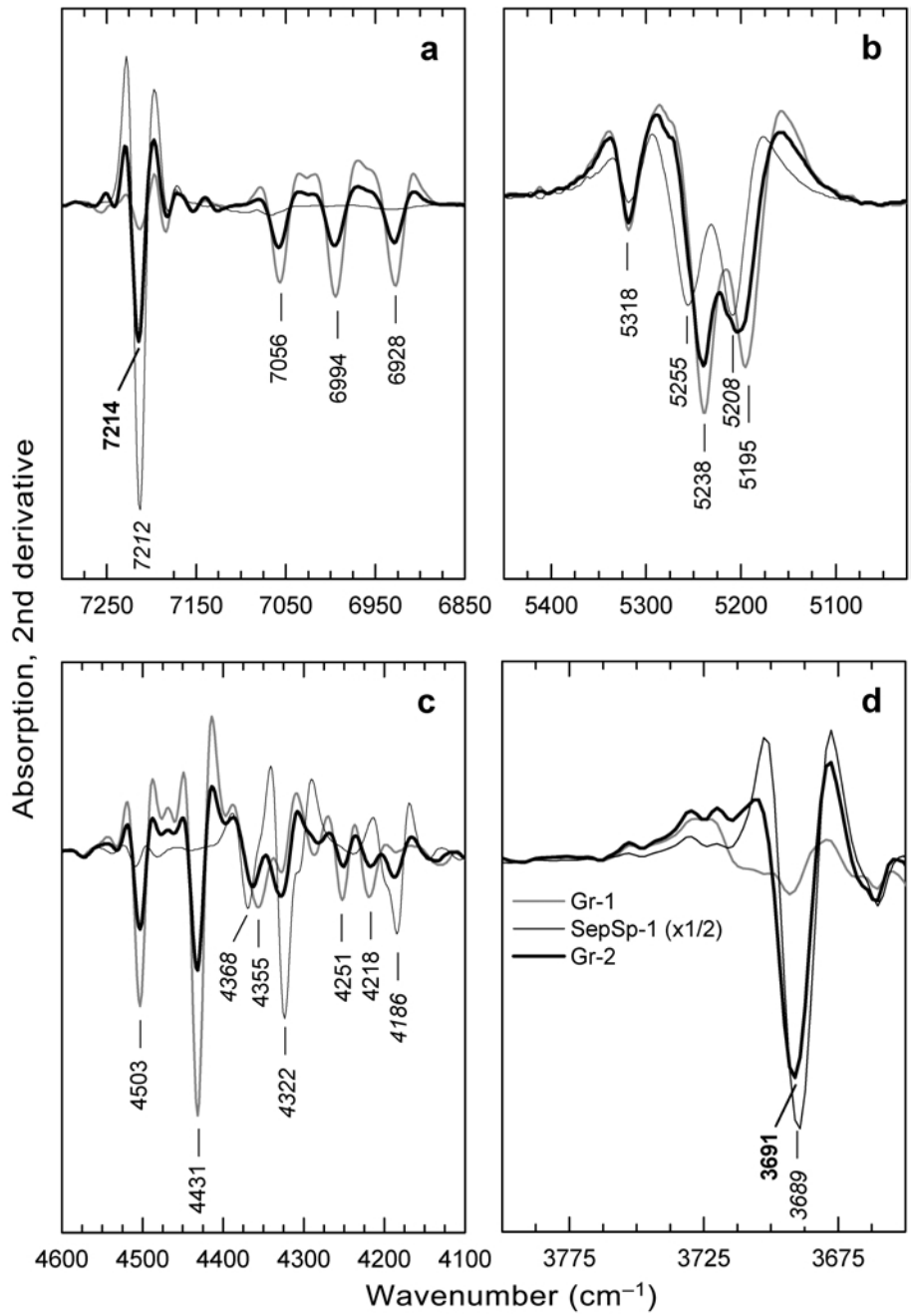

Figure 8. Details of 2nd derivative NIR spectra of Gr-2, in comparison to Gr-1 and SepSp-1. Depicted from a to d are the OH first overtone region, the H_2O combinations, the OH-stretching-bending and lattice combinations, as well as the upper OH-fundamental stretch frequency range, respectively.

square error of the prediction (RMSEP). In our case, we have performed three independent validations, using as test sets 1/3 of the total number of spectra selected randomly. All three independent validations were found to be optimized at 10 ranks, and predict palygorskite content with RMSEP = 4.2±0.1% and R^2 = 0.97±0.02 (Figure 10). Convergence was fast, and already at the 3-rank level the model fits the XRD data with RMSEP = 6.5 and R^2 = 0.94 (*cf.* Figure 9).

This significant correlation between NIR and XRD data allows for the quasi-independent use of NIR to estimate the palygorskite content of clay samples, as long as these samples contain little or no sepiolite. This correlation, together with the capability of NIR to identify independently the presence and speciation of the dioctahedral component, is of practical significance in the routine evaluation of palygorskite-containing clays.

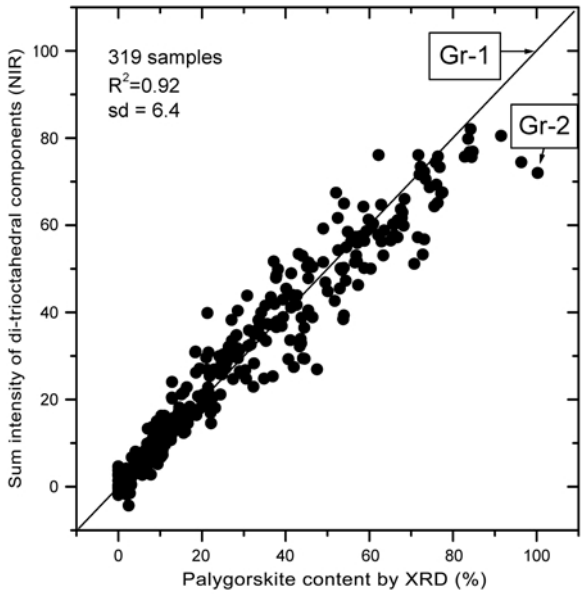

Figure 9. Correlation between the total (dioctahedral + trioctahedral) palygorskite contents of the Pefkaki samples estimated from the NIR and XRD data, and normalized to palygorskite Gr-1. For details see the text.

CONCLUSIONS

This work demonstrates that NIR spectroscopy can be used for the qualitative and quantitative evaluation of palygorskite in the presence of associated minerals, therefore providing a convenient means for exploring the compositional limits of palygorskite formation. Based on the study of more than 300 samples from the Pefkaki deposit in W. Macedonia, Greece, we confirm that dioctahedral palygorskite involves the vacancy of the inner octahedral *M*1 site and the occupation of the *M*2 sites by Al, substituted by up to 70% Fe^{III}. There is clear NIR evidence for the existence of $AlFe^{III}OH$, although the small relative fraction of this species suggests a preference for the formation of homoionic AlAlOH and $Fe^{III}Fe^{III}OH$ pairs. Trioctahedral palygorskite, with Mg atoms occupying triplets of *M*1*M*2*M*2 sites, is more difficult to identify by NIR at ambient conditions, because its characteristic Mg_3OH modes are very similar to those of sepiolite. The distinction between trioctahedral palygorskite and sepiolite is straightforward by XRD and TGA analysis. Our data suggest that TGA, and to some extent XRD, can distinguish between dioctahedral and trioctahedral-rich palygorskite from differences in the differential weight losses in the 200−250ºC range, as well as from small shifts of the 110 diffraction peaks, respectively. The generality of these observations requires validation with samples from other locations.

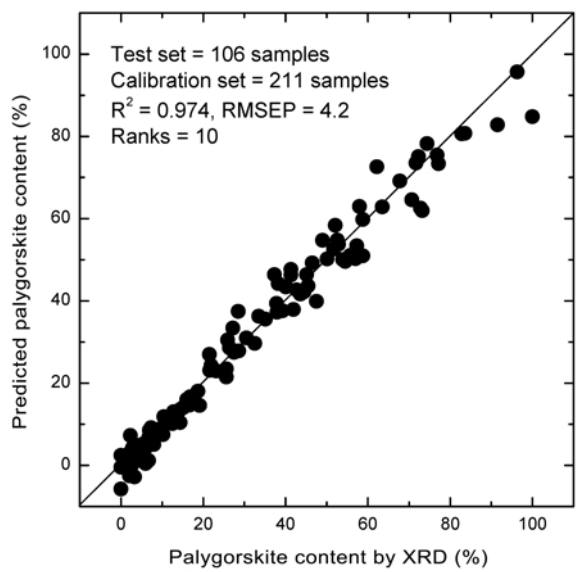

Figure 10. PLS chemometric prediction of total palygorskite content from the NIR spectra of the Pefkaki samples. For details see the text.

The trioctahedral palygorskite content can be estimated by measuring the deviations between the normalized intensity of the XRD peak near 10.4 Å and the sum intensity of the dioctahedral overtone modes in the NIR spectrum, or by comparing the intensity of the main Mg_3OH overtone at 7214 cm^{-1} with that of the corresponding band of SepSp-1. As a more appealing alternative, a PLS chemometric regression model has been built to predict the intensity of the 10.4 Å XRD peak from the NIR spectra of the Pefkaki samples. All three approaches suggest that trioctahedral palygorskite can account for up to ~55% of the total palygorskite content. This upper limit agrees well with published chemical analyses on single palygorskite particles from other locations. The fact that no fully trioctahedral specimen of palygorskite has ever been identified suggests that dioctahedral and trioctahedral entities must coexist in the same particle. However, the frequent alternation of dioctahedral and trioctahedral segments within the same slab (Chahi *et al.*, 2002) would create a large concentration of $M_2^{II}OH$ and $M_2^{III}M^{II}OH$ sites. The lack of spectroscopic evidence for these types of charged sites casts doubt on this model. Instead, the possibility that fully trioctahedral slabs can coexist with their dioctahedral analogs as oriented overgrowths of the type characterizing the palygorskite-to-smectite transformation (Krekeler *et al.*, 2005), or as regular intergrowths suggesting polysomatism (Ferraris and Gula, 2005) appears more plausible. These issues, as well as a correlation between the speciation of the octahedral sheet and the polytypism exhibited by palygorskite (Giustetto and Chiari, 2004) remain open for future research.

ACKNOWLEDGMENTS

The authors acknowledge the expert technical assistance of E. Typa, M. Drossos and E. Stathopoulou. Will Gates and Javier Cuadros are thanked for the many useful

comments they made when reviewing this manuscript. Research at TPCI/NHRF has been supported by an applied spectroscopy grant from Geohellas S.A.

REFERENCES

Artioli, G. and Galli, E. (1994) The crystal structures of orthorhombic and monoclinic palygorskite. *Materials Science Forum*, **166–169**, 647–652.

Brindley, G.W. and Brown, G. (1980) *Crystal Structures of Clay Minerals and their X-ray Identification*. Monograph, **5**, Mineralogical Society, London, pp. 104–115.

Cai, Y., Xue, J. and Polya, D.A. (2007) A Fourier transform infrared spectroscopic study of Mg-rich, Mg-poor and acid leached palygorskites. *Spectrochimica Acta Part A*, **66**, 282–288.

Chahi, A., Petit, S. and Decarreau, A. (2002) Infrared evidence of dioctahedral-trioctahedral site occupancy in palygorskite. *Clays and Clay Minerals*, **50**, 306–313.

Christ, C.L., Hathaway, J.C., Hostetler, P.B. and Shepard, A.O. (1969) Palygorskite: New X-ray data. *American Mineralogist*, **54**, 198–205.

Clark, R.N., King, T.V.V. , Klejwa, M., Swayze, G.A. and Vergo, N. (1990) High spectral resolution reflectance spectroscopy of minerals. *Journal of Geophysical Research*, **95**, 12653–12680.

Ferraris, G. and Gula, A. (2005) Polysomatic aspects of microporous minerals – heterophyllosilicates, palysepioles and rhodesite-related structures. Pp. 69–104 in: *Microporous and Mesoporous Phases* (G. Ferraris and S. Merlino, editors). Reviews in Mineralogy and Geochemistry, **57**. Mineralogical Society of America, Chantilly, Virginia, and the Geochemical Society, Washington, D.C.

Frost, R.L. and Ding, Z. (2003) Controlled thermal analysis and differential scanning calorimetry of sepiolites and palygorskites. *Thermochimica Acta*, **397**, 119–128.

Galán, E. and Carretero, I. (1999) A new approach to compositional limits for sepiolite and palygorskite. *Clays and Clay Minerals*, **47**, 399–409.

García-Romero, E., Suárez Barrios, M. and Bustillo Revuelta, M.A. (2004) Characteristics of a Mg-palygorskite in Miocene rocks, Madrid Basin (Spain). *Clays and Clay Minerals*, **52**, 484–494.

Gates, W.P. (2005) Infrared spectroscopy and the chemistry of dioctahedral smectites. Pp. 126–168 in: *The Application of Vibrational Spectroscopy to Clay Minerals and Layered Double Hydroxides* (T. Kloprogge, editor). Volume 13, CMS Workshop Series, The Clay Minerals Society, Chantilly, Virginia.

Gionis, V., Kacandes, G.H., Kastritis, I.D. and Chryssikos, G.D. (2006) On the structure of palygorskite by mid- and near-infrared spectroscopy. *American Mineralogist*, **91**, 1125–1133.

Giustetto, R. and Chiari, G. (2004) Crystal structure refinement of palygorskite from neutron powder diffraction. *European Journal of Mineralogy*, **16**, 521–532.

Güven, N., Caillerie, J.B.E. and Fripiat, J.J. (1992) The coordination of aluminum in the palygorskite structure. *Clays and Clay Minerals*, **40**, 457–461.

Heise, H.M. and Winzen, R. (2002) Chemometrics in near-infrared spectroscopy. Pp. 125–162 in: *Near-Infrared Spectroscopy: Principles, Instruments, Applications* (H.W. Siesler, Y. Ozaki, S. Kawata and H.M. Heise, editors). Wiley-VCH, New York.

Jones, B.F. and Galán, E. (1988) Sepiolite and palygorskite. Pp. 631–674 in: *Hydrous Phyllosilicates (exclusive of micas)* (S.W. Bailey, editor). Reviews in Mineralogy, **19**. Mineralogical Society of America, Washington, D.C.

Kastritis, I.D., Mposkos, E. and Kacandes, G.H. (2003) The palygorskite and Mg-Fe smectite clay deposits of the Ventzia basin, Western Macedonia, Greece. Pp. 891–894 in: *Mineral Exploration and Sustainable Development – Proceedings of the 7th SGA Meeting* (D. Eliopoulos *et al.*, editors). Millpress, Rotterdam, The Netherlands.

Krekeler, M.P.S., Hammerly, E., Rakovan, J. and Guggenheim, S. (2005) Microscopy studies of the palygorskite-to-smectite transformation. *Clays and Clay Minerals*, **53**, 92–99.

Madejová, J. and Komadel, P. (2005) Information available from infrared spectra of the fine fractions of bentonites. Pp. 66–98 in: *The Application of Vibrational Spectroscopy to Clay Minerals and Layered Double Hydroxides* (T. Kloprogge, editor). Volume **13**, CMS Workshop Series, The Clay Minerals Society, Chantilly, Virginia.

Martin Vivaldi, J.L. and Linares Gonzales, J. (1962) A random intergrowth of sepiolite and palygorskite. *Clays and Clay Minerals*, **9**, 592–602.

Moore, D.M. and Reynolds, R.C. Jr. (1997) *X-ray Diffraction and the Identification and Analysis of Clay Minerals*. Oxford University Press, New York, pp. 222–223

Paquet, H., Duplay, J., Valleron-Blanc, M.M. and Millot, G. (1985) Octahedral compositions of individual particles in smectite-palygorskite and smectite-sepiolite assemblages. *Proceedings of the International Clay Conference*, Denver, 1985 (L.G. Schultz, H. van Olphen and F.A. Mumpton, editors). The Clay Minerals Society, Bloomington, Indiana, pp. 73–77.

Petit, S., Robert, J.-L., Decarreau, A., Besson, G., Grauby, O. and Martin, F. (1995) Apport des méthodes spectroscopiques à la caractérisation des phyllosilicates 2:1. *Bulletin de Centre des Recherches Exploration-Production ELF-Aquitaine*, **19**, 119–147.

Petit, S., Decarreau, A., Martin, F. and Buchet, R. (2004) Refined relationship between the position of the fundamental OH stretching and the first overtones for clays. *Physics and Chemistry of Minerals*, **31**, 585–592.

Post, J.L. and Borer, L. (2000) High-resolution infrared spectra, physical properties, and micromorphology of serpentines. *Applied Clay Science*, **16**, 73–85.

Post, J.L. and Crawford, S. (2007) Varied forms of palygorskite and sepiolite from different geologic settings. *Applied Clay Science*, **36**, 232–244.

Post, J.E., Bish, D.L. and Heaney. P.J. (2007) Synchrotron powder X-ray diffraction study of the structure and dehydration behavior of sepiolite. *American Mineralogist*, **92**, 91–97.

Savitzky, A. and Golay, M.J.E. (1964) Smoothing and differentiation of data by simplified least-squares procedures. *Analytical Chemistry*, **36**, 1627–1639.

Singer, A. (1989) Palygorskite and sepiolite group minerals. Pp. 829–872 in: *Minerals in Soil Environments* (J.B. Dixon and S.B. Weed, editors). SSSA Book Series No. 1, chapter 17, Soil Science Society of America, Madison, Wisconsin.

Suárez, M. and García-Romero, E. (2006) FTIR spectroscopic study of palygorskite: Influence of the composition of the octahedral sheet. *Applied Clay Science*, **31**, 154–163.

Zviagina, B.B., McCarty, D.K., Środoń, J. and Drits, V.A. (2004) Interpretation of infrared spectra of dioctahedral smectites in the region of OH-stretching vibrations. *Clays and Clay Minerals*, **52**, 399–410.

(*Received 27 March 2007; revised 30 August 2007; Ms. 0007; A.E. Will P. Gates*)